Biochimica et Biophysica Acta, 984 (1989) 339–350
Elsevier

BBAMEM 74549

A possible model for the inner wall of the acetylcholine receptor channel

Sylvie Furois-Corbin and Alberte Pullman

Institut de Biologie Physico-Chimique, Laboratoire de Biochimie Théorique associé au CNRS, Paris (France)

(Received 11 January 1989)

Key words: Acetylcholine receptor; Channel conformation; Model membrane; Non-competitive blocker

A structural model of the inner wall of the acetylcholine receptor (AChR) channel is developed using assumptions derived from the results of the recent labelling experiments of the MII helices by noncompetitive blockers. The assumption of steric blocking of the channel by chlorpromazine (CPZ) in the neighbourhood of the labelled serines imposes the MII helices to be in contact at this level and allows the calculation of their minimal interaxial distance. The assumption that CPZ diffuses to this position through the upper crowded part of the channel imposes that the helices are more distant in this region and permits the determination of a tilt of about 7 degrees with respect to the central axis. Electrostatic potentials are used to demonstrate the effect of the charged residues at the exit of the pore. A discussion is given on the possible aptitude of MI to satisfy the contacts necessary with the MII/s at the different heights of the model.

Introduction

Due to the difficulty to obtain appropriately diffracting crystals of the acetylcholine receptor (AChR), there is not yet precise information on the three-dimensional structure of this membrane protein at atomic resolution. The available knowledge on its structural organization indicates that its four polypeptide chains α, β, γ and δ in the stoichiometry $\alpha_2\beta\gamma\delta$ [1–3], are arranged roughly regularly around a central axis with an approximate pentagonal symmetry [4–6] and in the clockwise order α β α γ δ (viewed from the extracellular side) [7]. Sequencing and amphipathy analysis [8–11] led to the concept that each subunit forms, in the membrane, a bundle of α-helices made by hydrophobic segments, various models having been proposed [12–15] for their number and organization around a central inner pore. In the presently prevalent view [16,17], each subunit possesses four membrane crossing segments MI to MIV, the disposition of which cannot be distinguished in the electron microscopic images [6].

Recent labelling experiments with non-competitive blockers (NCB) [18,19,14,5] and conductance measurements using chimaeras between the *Torpedo Californica* and the bovine AChR δ subunits [20] point strongly to the fact that the helices called MII, one MII in each subunit, contribute to the channel inner wall. Moreover, the identification of the labelled residues, homologous serines in the five MII helices at positions 248, 254, 257, 262, in α, β, γ, δ respectively, suggests that these residues essentially face the center of the inner pore [21,22] and, consequently, largely imposes the part of the MII helices which is turned towards the interior of the pore. We develop, in the present paper, a structural model of the channel inner wall based on conditions deduced from the implications of these results and compatible with the conductance properties of the receptor. In a preliminary study [23] we showed that, in order to satisfy the suggestion [19] that the high-affinity site of the non-competitive blocker chlorpromazine (CPZ) lies at the level, or in the neighbourhood, of the labelled serine residues, on the axis of quasi-symmetry of the $\alpha_2\beta\gamma\delta$ oligomer and at minimum distances to all five chains, consecutive MII helices must be laterally in contact at this level rather than separated by another helix. Satisfying this condition with five parallel MII helices in lateral contact we showed further that the lower part of the resulting pore from α Ser-252, β Ala-258, γ Ala-261, δ Ala-266 down to the N-terminus was wide enough to accommodate sterically the largest permeant ion, dimethyl diethanolammonium (DMDEA). Furthermore, calculations of the energy profile for DMDEA brought into evidence the decisive role in the

Correspondence: A. Pullman, Institut de Biologie Physico-Chimique, Laboratoire de Biochimie Théorique associé au CNRS, 13, rue Pierre et Marie Curie, 75005 Paris, France.

exit of the ion of the negatively charged glutamates situated at the N-terminal of the MII's, a finding strikingly confirmed since by site-directed mutation experiments [24].

In the exploration quoted, limited to the lower part of the channel, that containing essentially the most polar groups, we have announced that the resulting partial model needed to be refined and completed by taking into consideration the entire sequences of the MII helices as well as their possible inclinations. We present here the results of these investigations.

A possible model including the entire length of the MII helices

(a) Delimitation of the helices

We now consider the complete sequences of the five MII helices of *Torpedo marmorata*. The relevant hydrophobic segments and their alignment, taken from Ref. 11, are recalled in Fig. 1. Different limits have been proposed for the helices on the basis of hydropathy plots and/or charge considerations [11]. Concerning the lower limit we adopt the point of view suggested by the calculations on DMDEA and apparently confirmed by the site-directed mutation experiments of Ref. 24, namely that they start with the charged amino acids Glu-Lys (Gln-Lys in γ). These residues are consequently numbered 1 and 2 in the simplifying numbering indicated in Fig. 1.

Concerning the upper limits, we do not include in the helices the residues α Glu-262, β Asp-268, γ Gln-271, δ Gln-276, noting that, if the helices went further up, the presence of a proline in position 25 in our numbering, would produce a break (vide infra) at residue 21 by leaving a free non hydrogen-bonded carbonyl. Note that this carbonyl points upwards in the arrangement shown, thus towards the pore entrance.

(b) The necessity of a tilted arrangement of the MII helices

Let us consider first the overall shape of the arrangement of the five MII helices on the inner wall of the channel. We assume for simplicity that they are disposed symmetrically with respect to the center of the pore.

As recalled above, we have used in Ref. 23 the hypothesis deduced from the labelling experiments with tritiated NCB's, that the non-competitive blockers block the pore sterically at or in the neighbourhood of the labelled serine residues to demonstrate that the helices must be in contact at this level, and have built an *approximate* arrangement by setting them parallel at a distance of 10.5 Å. We now evaluate more precisely the minimal distance permitted for this contact.

On the other hand, to extend our modelling to the upper part of the pore we need information on their

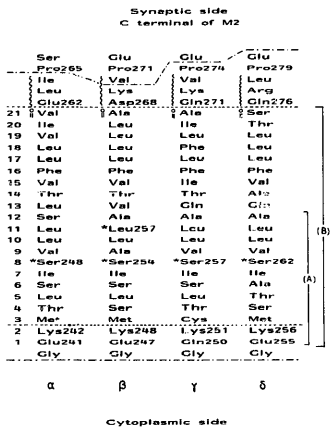

Fig. 1. The aligned sequences of the MII segments of *Torpedo marmorata* AChR. ·-·-·, limits of the MII helices according to Ref. 11. ·····, limits of the MII helices according to Ref. 10. (A) Portion investigated in Ref. 23. (B) Sequences involved in the present model. *, Residues labeled by ^{3}[H]CPZ [18,19] and ^{3}[H]TPMP [5,14] ⚲, free carbonyls (direction as indicated). }, region of probable bend. The numbering used in our computations is indicated in the first column. The other numbers correspond to the numbering used in the AChR aligned subunits sequences (see, for instance, Ref. 24).

minimal distance in this region. For this, we assume as a working hypothesis, that the non-competitive blocker approaches its high-affinity site [25] through the channel from the extracellular side. This implies that it must be accommodated, at least sterically, in the upper part of the pore. Examination of the sequences of Fig. 1 indicates that this section contains an appreciable number of bulky side chains. Among those, some will face the interior of the channel. If one admits on the basis of the labelling experiments that the labelled serines face the interior of the pore, a similar situation will hold (see the helix wheels of Fig. 2) for residue 15 in each helix, Val in α, β, δ and Ile in γ, as well as for residue 19, Val in α and Leu in β, γ, δ. It may be foretold that, for a constant interaxial distance of the helices, the side chains of these bulky residues would protrude much more into the pore than the side chains of the serine, leaving thus a narrower free space in their part of the channel. An approximate evaluation of the space occupied by these residues was performed by energy optimization (see

TABLE I

Distance (d, in Å) to the axis of the most external atom of the X (X = Ile, Leu, Val or Ser) side chain for the most retracted (I) and the most extended (II) conformations of X, in a $COCH_3(Ala)_4X(Ala)_4NHCH_3$ optimized α-helix (φ, ψ fixed at their standard values of Ref. 30)

Dihedral angles (χ_i, in degrees) defined according to the IUPAC-IUB (1970) convention (for Ile χ_2 stands for $\chi_{2,1}$, χ_3 for $\chi_{2,2}$ and χ_4 for $\chi_{3,1}$). Only one conformation is allowed for Val in the tested α-helix, all others leading to close contacts between the side-chain and the helix backbone.

	(I)					(II)				
	d	χ_1	χ_2	χ_3	χ_4	*d*	χ_1	χ_2	χ_3	χ_4
Ile	5.78	−73.7	166.5	52.2	73.4	5.99	−71.8	−77.1	45.1	48.4
Leu	6.24	−78.9	158.0	54.2	59.7	6.63	−173.3	136.3	58.4	60.7
Val	5.24	166.4	48.2	55.8		5.24	166.4	48.2	55.8	
Ser	4.06	−65.3	76.1			5.11	−176.2	−176.5		

Appendix) (using a large number of starting conformations) of the most extended and most retracted (with respect to the helix axis) allowed conformations of the residue *X* (for *X* = Val, Ile, Leu and Ser) in an α-helical sequence $COCH_3$-$(Ala)_4$ -*X*- $(Ala)_4$-$NHCH_3$, and the corresponding distance to the helical axis of the most external side chain atom was determined. The resulting values (Table I) show clearly that the side chains of Leu, Val and Ile do indeed fill a larger space than that of Ser in a similar situation.

Therefore if the non competitive blocker is at a contact distance of the five MII's at the level of the labelled serines, it would feel steric hindrance in the upper part of the pore if the helices were parallel. We have verified this situation on our graphic terminal using the real MII sequences by explicit computations of Van der Waals contacts (see Appendix) using different possible conformations for CPZ.

The necessity to relieve this steric hindrance in the upper part of the channel while maintaining the appropriate minimal diameter at the level of the labelled serines *imposes* thus a model where the helices are *tilted*, forming a truncated conical structure, with the largest spacing at the top. The arguments developed above allow an explicit determination of the width of the transmembrane part of the pore at different levels.

(c) Determination of the minimal dimensions of the inner pore

The dimensions of the truncated cone delimited by the five MII helices satisfying the conditions stated above have been determined in a first approximation

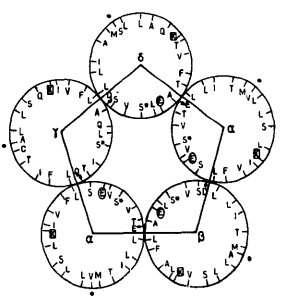

Fig. 2. Projection, onto the plane perpendicular to the helical axis, of the C_α atoms of the MII helices surrounding the pore. The α-helical structure starts with the Glu(Gln in γ) residues following the common Gly in the sequences of Fig. 1. The Ser residues labelled by the NCB are noted by a star and placed in a completely symmetric fashion facing the central axis. The Glu(Gln) at the N-terminal are noted by an oval, the following Lys by a rectangle. The 21st residue indicated by a fat dot carries a free carbonyl. The position of the C_α of the residue following it is shown by an arrow.

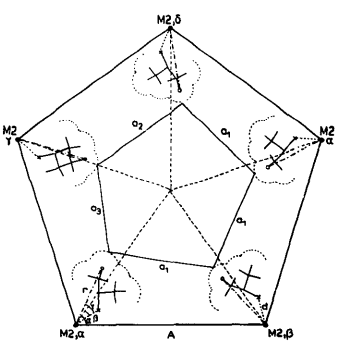

Fig. 3. Geometrical construction used to allow an estimation of the inner free space available at the level of the residue considered (example given for residue 15). ●, helical axis of the MII α-helices. *x*, C_α atom of residue *X*. ○, most external atom of the side-chain of residue *X* (Val in α, β, δ, Ile in γ) taken in a given conformation.), Van der Waals envelope of the involved side-chain.

using geometrical considerations. Fig. 3 and its caption indicate the geometrical elements intervening in the computations. The figure is drawn in the most general case in a plane perpendicular to the central axis at the height corresponding to the α carbons of the residues considered. (When these residues are the serines 8, assumed for simplicity to point exactly towards the central axis, the α carbons are along the bisector of the angles of the regular pentagon delimited by the traces of the five helical axes on the plane). Three levels were considered: first that of the labelled serines, to obtain the minimal distance compatible with a pore dimension barely accommodating sterically CPZ (keeping it just in contact with the five MII helices); then, the levels of residues 15 and 19, respectively, to obtain the minimal distance between the helices producing a pore wide enough to accommodate CPZ without contact at both levels. Using the projections onto the plane of the most external atoms of the five side chains considered and taking into account their Van der Waals radii, permits to draw the limits of the inner pentagon defining the hole for the conformation considered. Simple geometry relations existing between the angles α, β, γ, the distances r, d, and the tilt angle of the helices permit to express the distances a_i in the inner pentagon in terms of the interaxial distance A between two adjacent MII's and thus to find the value of A compatible with the dimensions imposed by the size of CPZ. We used on the one hand the geometry corresponding to the available crystal structure of CPZ [26], and also, a conformation obtained by energy optimization where the molecule fills a smaller space, perpendicularly to the channel axis, than in the crystal structure.

This preliminary search led to a set of values of the distance A between the helices at different levels which allowed us to build several bundles. In fact, in these bundles, we accounted for the experimental result [21] that in MII of the β subunit both Ser-254 and Leu-257 are labelled by ^{3}[H]CPZ, by slightly rotating this helix around its helical axis so as to bring both Ser-254 and Leu-257 to face the channel interior. These bundles were then submitted to a more thorough examination on our interactive graphic terminal coupled with energy calculations of their Lennard-Jones interaction (see Appendix) with CPZ placed at different heights within the pore, with the average plane of its ring perpendicular to the channel axis, in different orientations.

Extensive examination of a large number of bundles in this fashion finally led to the acceptable structure reproduced in Fig. 4. In this structure the distances between the axes of two adjacent MII helices go from 10 Å at the level of the α carbons of the first residue (Glu in α, β, δ, Gln in γ) to 14.2 Å at the level of the α carbons of the 21st residue (Val in α, Ala in β and γ, Ser in δ). It is 11.5 Å at the level of the labelled serine residues, becoming 13.0 and 13.75 Å at the level of residues 15 and 19, respectively. With these dimensions the atom-atom contacts at all levels satisfy the conditions imposed (see Table II). It is observed that at the level of residues 15 (Val or Ile), an increase of the interatomic distance by 0.1 Å would suffice to remove the contact observed: this can easily be achieved by a slight change in the relevant aminoacid side-chain conformation (all side-chain conformations are taken here from Ref. 27) or a slight rotation of the helix involved. This is true also for the contact found at the level of the labelled serines. In that case, however, CPZ is at the permitted minimal distance of the five helices: immediately below much stronger contacts exist.

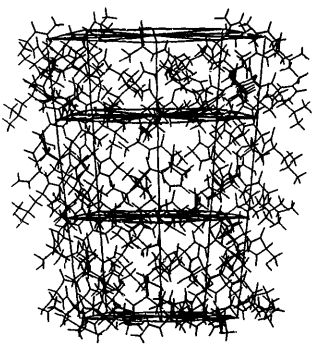

Fig. 4. The truncated cone formed by the five MII helices in the model. The pentagons are drawn to facilitate viewing at C_α of residues 1, 8, 15 and 21.

The dimensions obtained correspond to a tilt of the five helices of about 7 degrees with respect to the

TABLE II

Characteristics of the positions of CPZ at different levels in the channel

The average height of the atoms of the CPZ ring system is the same, within the channel, than that of the C_α atoms of the residues indicated (according to the numbering shown in Fig. 1). $E_{LJ}(i, j)$ (kcal.mol) is the (dispersion+repulsion) component (see text) of the interaction energy between atom i on CPZ and atom j belonging to the MII helix indicated. H(X) is one hydrogen atom bound to X; designation of the amino-acid side-chains atoms following the IUPAC-IUB (1970) convention. r_{ij} (Å), interatomic distance between i and j. r^{min} (Å), minimal distance at which there is no more close contact between i and j.

C_α	$E_{LJ}(i, j)$	i	j	r_{ij}	r^{min}
19	1.84	H(C10)	H($C_{\delta 2}$) Leu_{19}, MII_γ	1.95	1.81
15	10.4	H(C2)	H($C_{\gamma 2}$) Val_{15}, MII_β	1.71	1.81
9	8.5	H(C2)	H(C_β) Ser_8, $MII_{\alpha 1}$	1.74	1.81

TABLE III

The six first conformations, in order of decreasing stability, resulting from energy optimization of a $COCH_3(Ala)_4GluLys(Ala)_4NHCH_3$ α-helix (ϕ, ψ fixed at their standard value of Ref. 30

E, conformational energy (in kcal/mol) with respect to that of the most stable structure. $r = H \cdots Q$ (Ångströms) for the interaction $PH \cdots Q$, θ = (PH, HQ) in degrees. Dihedral angles (χ, degrees) according to the IUPAC-IUB (1970) convention. $H(N_\zeta)$ is one of the hydrogen atoms of the NH_3 group of Lys; O(C′) is a peptide carbonyl oxygen.

E	Salt bridge	Involved atoms				*r*	θ	Side-chain conformation							
								Glu				Lys			
								χ_1	χ_2	χ_3		χ_1	χ_2	χ_3	χ_4	χ_5
0.0	yes	Glu	O_1	Lys	$H(N_\zeta)$	1.75	12.9	171.5	−93.9	−44.1		−76.8	−82.1	−153.1	−80.5	77.8
2.3	yes	Glu	O_1	Lys	$H(N_\zeta)$	1.74	9.6	176.5	−101.9	−75.6		−102.6	76.0	−161.8	91.3	65.3
4.3	yes	Glu	O_2	Lys	$H(N_\zeta)$	1.69	3.8	177.0	−98.3	−58.4		−126.2	63.8	−123.0	157.5	44.6
4.7	yes	Glu	O_2	Lys	$H(N_\zeta)$	1.77	13.2	174.7	−116.1	−53.0		−106.8	64.2	−159.7	155.5	61.4
11.2	no							−169.5	−97.7	−76.4		−70.2	−57.7	107.5	−149.5	56.1
30.7	H bond	Ala	O(C′)	Lys	$H(N_\zeta)$	2.02	26.9	−66.2	152.6	162.9		−103.3	88.2	−92.2	161.6	68.7

central axis considered vertical. With these dimensions the helices are in close contact at their bottom and up to about the level of the labelled serines, above which the close imbrications become looser, slowly beginning to leave a gap between the helices, gap which widens up to the top. We shall come back to this situation in point (e) below. Concerning the lower part of the present model, we have tested that the conclusions obtained in [23] remain valid, namely that it accommodates easily the largest permeant ion DMDEA even in its narrowest part.

Let us consider in more details the structure at the low end of the model and its significance.

(d) The exit of the channel and the role of the charged residues at the end

As recalled earlier, we have included at the N-terminal of the MII helices the Glu-Lys residues (Gln-Lys in γ) since their presence has proven instrumental in providing the attraction necessary to help the cation exit the pore. This is due to the fact that the inclusion of these residues within the helical stretch forces the negatively charged residues to face the interior of the pore while the positively charged lysines face the external side of the helix (see the helical wheels of Fig. 2).

These apparently distant locations do not preclude, however, the possibility for the two residues to use their long side chains for the formation of a salt bridge in a configuration where the Glu(Gln) side chain curls up towards the side chain of the following lysine. The feasibility and stability of such n, $n+1$ bridges was examined by energy minimization (see Appendix) of the two following α-helices:

S1: $COCH_3$-(Ala)$_4$-Glu-Lys-(Ala)$_4$-$NHCH_3$

S2: $COCH_3$-(Ala)$_4$-Gln-Lys-(Ala)$_4$-$NHCH_3$

using as starting conformations of the Glu(Gln) and Lys side chains those given in the conformer library of Ref. 27. 49 different structures of S1 and of S2 were optimized, labilizing all the side chain dihedral angles while keeping the backbone dihedral angles at their standard α-helical values [28]. The results, indicated in Table III, show that the most stable conformation of S1 involves a strong salt bridge between the extremity of the side chain of Glu and that of Lys, whereas the next

TABLE IV

The six first conformations, in order of decreasing stability, resulting from energy optimization of a $COCH_3(Ala)_4GlnLys(Ala)_4NHCH_3$ α-helix (ϕ, ψ as in Table III)

Conventions as in Table III; $H(N_{\varepsilon 2})$ is one of the hydrogen atoms of the Gln NH_2 group.

E	H bond	Involved atoms				*r*	θ	Side-chain conformation								
								Gln				Lys				
								χ_1	χ_2	χ_3	χ_4	χ_1	χ_2	χ_3	χ_4	χ_5
0.0	yes	Gln	O_1	Lys	$H(N_\zeta)$	1.96	14.2	178.7	−165.5	79.8	−179.1	−101.4	66.2	−166.3	176.6	65.2
1.1	no							−74.3	173.7	−96.3	179.6	171.5	58.2	172.7	168.1	57.9
1.2	no							−174.5	−179.8	98.2	−179.6	173.1	57.9	171.2	169.3	58.0
1.8	no							−74.3	172.8	−98.8	179.6	−170.8	−98.4	165.6	−174.2	60.4
2.8	yes	Gln	O_1	Gln	$H(N_{\varepsilon 2})$	2.21	37.8	−179.8	63.3	82.5	−178.2	171.8	58.4	172.2	168.9	58.0
3.3	no							−175.2	177.6	95.8	−179.5	−169.8	−98.0	165.4	−174.7	60.1

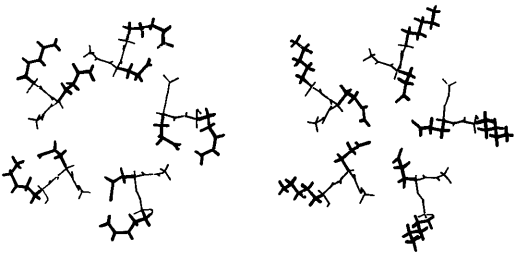

Fig. 5. The free space at the N-terminal of the bundle of Fig. 4: (a) when the charged residues form salt bridges; (b) when they are free in a more extended conformation (see text).

stable conformation which does not involve a salt bridge is by far less stable (line 5 in Table III). These results are in good correlation with the conclusions of a survey [29] of the α-helical segments in 47 globular proteins, showing that the occurrence of a Glu-Lys ion pair of the $n,n+1$ type follows immediately in frequency that of the predominant $n,n+4$ type, an indication of an appreciable intrinsic propensity of this conformation. In the case of the S2 helices (Table IV) the most stable state involves a strong hydrogen bond between the end of the Gln side chain and that of the charged lysine following it. These overall results support the hypothesis that a similar situation can occur in the MII helices considered here. The corresponding salt bridges were in fact constructed in [23] using the real sequences of the lower half of the MII's and shown in the energy minimization, to allow stable structures with no close contact between their atoms and the rest of the structure.

Despite the fact that other conformations of these Glu(Gln)-Lys groups might be imagined, their inclusion in the helix and their folding in bridges has the advantage of avoiding the problem raised in Ref. 30 of steric hindrance caused by the (assumed) floating of the Glu side chains towards the center of the pore: Fig. 5 shows clearly the difference in the size of the inner space enclosed by the helices (seen from their C-terminal extremity) when the Glu(Gln)-Lys residues are in a salt bridge conformation and when the Glu(Gln) extend towards the center of the channel. In the last case, DMDEA would indeed encounter a large steric hindrance to exit while it can pass easily in the first case. Furthermore, not only can the ion pass easily from the sterical point of view, but also, as demonstrated in Ref. 23, from the energetical point of view, since the field created by the ring of glutamates, even involved in salt bridges as indicated above, is sufficient to favor the exit. This is possible because, as stressed earlier, the α-helical structure, together with the internal positions of the labelled serines imposes the location of the negatively charged residues on the internal face of the helix, with the positively charged residues on the opposite side. The formation of salt bridge brings about only a partial neutralization and an asymmetry of the charge remains with the negative end closer to the pore, thereby acting favorably on the cation.

A pictorial demonstration of these effects is given in Fig. 6 showing the electrostatic potentials created by the bundle of MII helices placed as in Fig. 4, in a plane containing the C_α's of Thr-244 and homologs (thus, near the *exit* of the channel). When the Gly-Lys (Gln-Lys) are not included in the α-helices, the potentials (Fig. 6a) are everywhere strongly positive (repulsive for a cation). When these two residues are included (Fig. 6b) these potentials decrease strongly in a wide area of the inner region, a result due to the proximity of the negative glutamates. At the same time, the potentials in the exterior part of the helices become still more positive than in Fig. 6a, clearly indicating the effect of the lysines closer to the exterior. Note that a strong positive potential remains in the inner region facing the Gln of subunit γ, a reflection of the remaining dominance of the Lys positive charge less well compensated in this salt bridge than in the four others.

The site-directed mutation experiments of Ref. 24 confirm entirely these conclusions and our underlying hypotheses: (i) mutating the negatively charged residues at the level considered (intermediate ring in the notations of Ref. 24) has the strongest effect on the conductance, showing that they are close to the pore and closer than any other negatively charged residue; (ii) the ab-

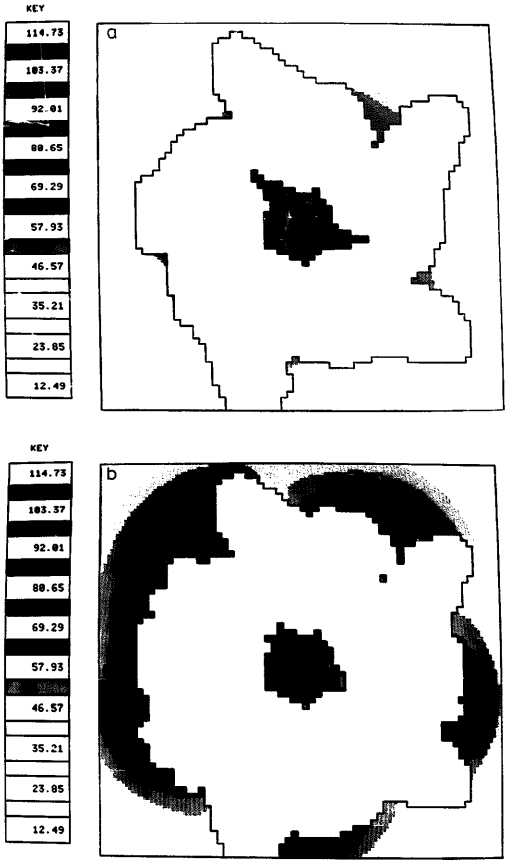

Fig. 6. Maps of the electrostatic potential created by the ensemble of the five MII helices in a plane situated near the exit of the pore about the level of α Thr-244. Scale of shading as indicated, in the left side, in kcal/mol. Contour lines: the potentials are interrupted at 2 Å from the atoms intersecting the plane studied. (a) Glu-Lys (Gln-Lys in γ) at the N-terminal not included in calculation. (b) Glu-Lys (Gln-Lys in γ) at the N-terminal included in calculation.

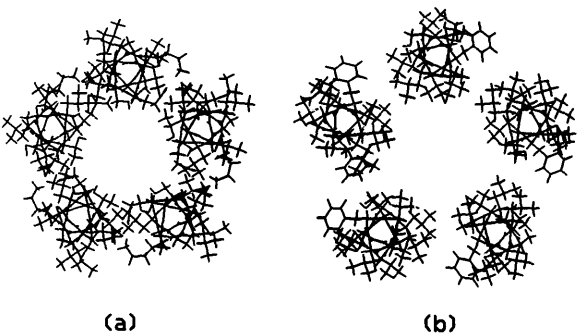

Fig. 7. (a) The lower part of the truncated cone of MII helices seen along the axis of the cone from the twelfth residue down to the N-terminal. (b) The upper part of the same cone seen from the C-terminal.

sence of effect seen when mutating the positively charged residues at the adjacent position in the sequence peaks in favor of their being on the outer side. These findings favor the hypothesis adopted that the Glu-Lys (Gln-Lys) residues at this level are part of the helix and disposed as indicated. They also confirm the location of α Glu-262 and homologs as indicated in section (a) above: their location just after the last residue of the helical structure can still impose the location of their C_α only as indicated in the helix wheels of Fig. 2, but farther from the symmetry axis than α Glu-241 and its homologs.

(e) The gaps between the MII helices on the inner wall and the possible role of MI

In the model described above, the interaxial distances between the adjacent MII helices at the different levels show that they are in close interaction at the lower level and up to the neighbourhood of the labelled serines. Further up, a very small gap between them appears which widens towards the top of the pore where, however, the distance between two adjacent helices does not exceed 14.2 Å. The free space is relatively small (see Fig. 7), anyway insufficient to allow the complete insertion of another helix (even a partial insertion [23] requires a minimal distance of at least 14.6 Å between two consecutive MII helices). In fact, in the present model, a simple contact with another helix in the gap region is sufficient to insure the tightness of the wall as well as the stability of the packing.

Overall the small tilt of the helices suggests that the contact with the outer helix occurs as schematized in Fig. 8a in the neighbourhood of the high-affinity site of the non-competitive blocker, and as in Fig. 8b in the 'gap' region: if we assume that each subunit participates in the transmembrane structure by the four hydrophobic helices MI-MIV, one may attempt to specify further which of the helices of each subunit plays the role of the contact helix in Fig. 8. From the point of view of proximity, MI or MIII which are separated from MII by relatively short segments, are good candidates, while MIV could be further away. (The exposure to the lipid of MIV in *Torpedo marmorata* is supported by its labelling by photoreactive markers in PC heads [31]).

A role for helix MI in the channel wall is sometimes suggested (see for example, Refs. 30 and 32) on the basis that labelling of this helix by the non-competitive blocker quinacrine azide was reported [33,34] although not confirmed or explicited.

Another feature pointing to a special role for the hydrophobic segment MI, underlined initially by Noda et al. [10] resides in the presence in this segment of three strikingly conserved proline residues at homologous

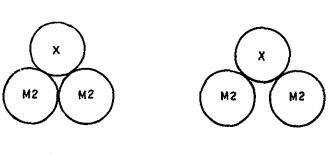

Fig. 8. Mutual disposition of two adjacent MII helices and another helix (a) lower part of the channel; (b) upper part of the channel (see text). The view is schematic.

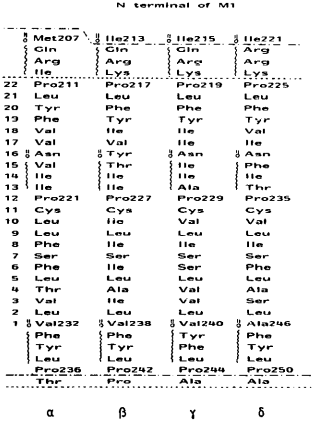

Fig. 9. The aligned sequences of the MI helices of *Torpedo marmorata* AChR. ·-·-·, limits of the MI helices according to Ref. 11. ·····, limits of the MI helices according to Ref. 10. ⇕, free carbonyls (direction as indicated). ⟆, region of probable bend. The numbering on the left side refers to the residues included in MI aligned to those of MII (see text). Beware of the opposite senses of MI and MII on the figures.

positions in the four subunits, one on the side of the N-terminal, Pro-211, Pro-217, Pro-219, Pro-225 in α, β, γ,δ, respectively; Pro-221, -227, -229, -235 in the same order ten residues further, and Pro-236, -242, -244, -250 similarly, in the C-terminal region (see Fig. 9 for a reminder of the sequences of segment MI in the four subunits). In view of recent inaccurate statements (see, for example, Refs. 32 and 35) on the effect of such prolines it is not superfluous to restate the situation briefly: proline residues produce 'kinks' in α-helical structures due first to the fact that they lack one free NH bond for hydrogen bonding to the carbonyl oxygen normally situated four residues below in the helix on the N-terminal side, second to the steric crowding produced by the structure of the residue itself, which interferes in particular with the carbonyl group of the residue situated three positions down in the sequence Recent energy optimizations [36,37] show explicitly how a 'bend' occurs in the helical structure by changes in the dihedral angles intervening between the proline-*n* and the $(n-4)$th residue left with a free carbonyl, a regular α-helical structure being essentially reestablished from the proline up towards the C-terminal.

The incidence of this effect on the hydrophobic segments MI is indicated formally in Fig. 9 showing the positions of the non hydrogen-bonded carbonyls (at Met-207, Ile-213, Ile-215, Ile-221, at Asn-217, Tyr-223, Asn-225, Asn-231 and at Val-232, Val-238, Val-240, Ala-246) and of the consecutive probable bends in the three regions between the *n*th proline and the $(n-4)$th residue. This analysis leads to a plausible assignment of the N- and C terminals of helix MI and of its possible role in comparison to that of MII.

Concerning the C-terminal, it appears reasonable to assume that the bend initiates the necessary curvature of the 'loop' intermediate between MI and MII. This, together with our hypothesis that the helices MII extend to Glu-247 in α and equivalent positions in the other subunits, ensures a reasonable length to this loop, setting the C-terminal limit of the helical segments MI at Val-232 in α and homologs in β, γ and δ, with a free carbonyl group pointing towards the cytoplasmic side. Such a carbonyl could play a role in the interaction with ions and/or water, or another side chain of the loop (see also Ref. 35).

Concerning the N-terminal limit of MI, there is at the moment no evidence that it includes residues preceding Pro-211 in α (Pro-217, Pro-219 and Pro-225 in β, γ, δ). At any rate, the α-helical stretch would be interrupted at α Met-207, β Ile-213, γ Ile-215 and δ Ile-221 four residues before Pro-211 and its homologs with an intermediary bend apt to make the connection with the extracellular segment. (It is for the same reason that we have interrupted the MII helices after α Val-261, β Ala-267, γ Ala-270 and δ Ser-275; α Glu-262, β Asp-268, γ Gln-271 and δ Gln-276, initiating, respectively, the loop between MII and MIII in each subunit).

With the limits defined in this fashion the helical portion of MI includes thus 22 residues, only one more than the helical portion of MII defined earlier. Hence MI and MII can be conceived as spanning essentially the same transmembrane width, all the more so since MI is necessarily somewhat bent. Calculations on the details on the various bends in the AChR helices will be given elsewhere. To illustrate briefly the possible situation created by a proline in its neighbourhood, we give simply here the results of energy optimization upon labilizing all the dihedral angles including the proline ring (see Appendix) on the portion of MI of subunit α which contains the internal proline-221, considering the real sequence Asn-Val-Ile-Ile-Pro-Cys (from N- to C-terminal) embedded in an α-helix made otherwise of alanines. Using different energy-minimization pathways, the most stable structure obtained described in Table V by the values of the backbone dihedral angles ϕ, ψ, and ω and the characteristics of the hydrogen

TABLE V

Characteristics of the backbone hydrogen bonds O(C') –H(N) and values (in degrees) of the backbone dihedral angles in an optimized $COCH_3(Ala)_4$-Asn-Val-Ile-Ile-Pro-Cys-(Ala)$_4$-NHCH sequence starting from an α helix

$d = d$(O ··· H) in Ångströms; θ = (NH, HO) in degrees.

Backbone hydrogen bonds				Backbone dihedral angles			
Residues		d	θ	Residues	ϕ	ψ	ω
Ac ··· Ala_4		1.98	8.5	Ala_1	−57.8	−48.2	−179.6
Ala_1 ··· Asn_5		2.00	11.9	Ala_2	−55.0	−50.5	−176.0
Ala_2 ··· Val_6		2.12	19.3	Ala_3	−58.6	−49.9	−178.4
Ala_3	Ile_7	1.96	19.2	Ala_4	−55.3	−50.5	−175.0
Ala_4	Ile_8	1.99	3.4	Asn_5	−57.1	−43.4	−178.8
Asn_5	Pro_9	no H-bond		Val_6	−64.9	−52.4	−165.9
Val_6	Cys_{10}	no H-bond		Ile_7	−70.8	−60.2	−153.5
Ile_7	Ala_{11}	1.96	13.0	Ile_8	−59.4	−57.9	−169.9
Ile_8	Ala_{12}	1.98	14.3	Pro_9	−61.0	−55.8	−176.3
Pro_9	Ala_{13}	1.97	12.8	Cys_{10}	−55.9	−47.8	−175.6
Cys_{10}	Ala_{14}	1.98	13.9	Ala_{11}	−59.6	−47.9	−177.0
Ala_{11}	($NHCH_3$)	1.96	8.7	Ala_{12}	−61.8	−46.6	−176.4
				Ala_{13}	−60.9	−45.1	−179.3
				Ala_{14}	−62.2	−48.2	178.5

bond network, indicates clearly that the helix is somewhat bent from Asn-5 up to Pro-9: beside the lack of the Asn-5 ··· Pro-9 hydrogen bond, due to the absence of the hydrogen atom on the nitrogen of the proline, another lack in the α-helical hydrogen-bond network is observed between Val-6 and Cys-10. Interestingly, this is replaced by the formation of a hydrogen bond between the peptide carbonyl oxygen of Val-6 and the hydrogen atom bound to the sulfur of Cys-10. The fact that a cysteine residue is present at the same position after the proline in all MI segments in the AChR indicates a possible importance of this structural feature. The values of ϕ and ψ, in the α-helical domain up to Asn-5, deviate appreciably from the standard values ($(\phi, \psi) = (-57°, -47°)$ [28]) from Val-6 to Pro-9. From Cys-10 onwards, ϕ and ψ have recovered α-helical values. These calculations illustrate the essential structural features of the situation which can be created by the proline residue in its neighborhood for the particular sequence involved. The consequences of these features on the lability of helix MI and on its interaction properties with the other helices, particularly MII, must be ascertained by explicit calculations. It is however, interesting that if one adopts our proposed limits for MI and the alignment of its C-terminal with the N-terminal of MII (numbering of Figs. 1 and 9), the calculated bend coincides with the region where the separation of the adjacent MII's become detectable in our cone-shaped model, possibly facilitating the appropriate packing of the helices at different heights.

Concluding remarks

Adopting the assumption based on the labelling of the serine residues 248 in α, 254 in β, 257 in γ and 262 in δ that the MII hydrophobic segments are organized as α-helices around the pore in a pentagonal arrangement with the labelled serines facing the interior, we have shown that:

(a) the notion that CPZ is at minimal distances to all five chains at or in the vicinity of the labelled serines imposes that adjacent MII helices are in contact with each other, with a minimal interaxial distance of about 11.5 Å at the level of the α carbons of the labelled serines;

(b) if the five helices adopt this interaxial distance along their entire length, the bulky side chains lining the upper part of the pore preclude diffusion of large permeants or NCB's through this part. For such diffusion to occur, the MII helices must be tilted. The minimal dimensions computed to allow free passage of CPZ correspond to a tilt of about 7 degrees of each MII helix with respect to the central axis in an assumed regular arrangement;

(c) the resulting bundle allows free passage of DMDEA in its lowest narrow portion;

(d) energy profiles and molecular electrostatic potentials show that the negatively charged residues α Glu-241 and its homologs are of determining importance for insuring the *exit* of the cation;

(e) the relatively small tilt of the MII helices in the proposed model generates only a small gap in the upper part of the pore wall, which can be easily closed by contact with a single other helix;

(f) the reassignment of the extension of the helical part of the MI hydrophobic segments on the basis of the properties imposed by their three conserved proline residues leads to limit their length to 22 residues, with an intermediary bend. This length and the location of the bend can possibly help the MI segments to insure

the necessary contact at the different heights of the truncated cone of MII helices.

At this point a few remarks are in order: concerning point (a), a referee suggested that the binding of CPZ at the level of the labelled serines may be reactivity- rather than sterically controlled. There is at present no experimental evidence one way or the other. However, the 'contact' argument which we have used is valid whatever the events which occur after contact (in order to react the reagents must first be in contact). Too little is known at present concerning the nature of the reagents after irradiation for going beyond this by theory. A theoretical study of the behavior observed [38] with the NCB QX222 in the native and mutated channel will perhaps bring new insights in this connection.

Another remark concerns the truncated conical structure obtained for the channel. We have shown that it results from the structural features of the helices and from our basic assumptions. This is not the same as imposing the tilt [30] on the (very approximate) basis of the 'funnel' shape of the extramembranar part of the receptor seen in the electron microscopic image. The small tilt found in the model is compatible with the funnel but not imposed by it.

The resulting model is compatible with the known experimental features and allows a clear rationalization of the role of the charged residues situated at the N- and C-terminals of the MII helices. As it is, we hope that it can provide an inspiration for further experimental and theoretical investigations.

Appendix

The conformational studies of the α-helical sequences $COCH_3$-$(Ala)_4$-*X*-$(Ala)_4$-$NHCH_3$, where *X* is Val, Ile, Leu or Ser, and $COCH_3$-$(Ala)_4$-*Y*-Lys-$(Ala)_4$-$NHCH_3$, where *Y* is Glu or Gln, have been carried out using the energy minimiziation technique developed in our laboratory [39]. The method being described in detail in Ref. 39, we only recall here its essential.

The energy formula is given by the following equation:

$$E = \sum_{ij^*} \frac{q_i q_j}{r_{ij}} + \sum_{ij^*} \left(\frac{-A_{ij}}{r_{ij}^6} + \frac{B_{ij}}{r_{ij}^{12}} \right) + \sum_S \frac{V_S}{2} [1 \pm \cos(n_S \tau_S)] \qquad \text{(A-1)}$$

The first term represents the electrostatic energy computed for an assembly of atomic charges *q*, summed over all pairs of atoms *ij** separated by at least three chemical bonds. The charges are optimized atomic monopoles reparametrized [40] from the Hückel-Del Re [41,42] procedure so as to reproduce to very good accuracy the electrostatic potential and field surrounding the protein constituents (the peptide backbone and the different amino acid side-chains), in different conformations.

The second term corresponds to the sum of the dispersion and repulsion energies treated as a Lennard-Jones interaction with the conventional 6–12 distance dependence, the parameters *A* and *B* originating from Zhurkin et al. [43] and extended [39]. Furthermore, to account for the angular dependence of hydrogen bonds interactions, the second term of Eqn. A-1 becomes:

$$\sum_{ij\text{-H-bonded}} = \left[\cos\theta \left(\frac{-A_{ij}^{HB}}{r_{ij}^6} + \frac{B_{ij}^{HB}}{r_{ij}^{12}} \right) + (1 - \cos\theta) \left(-\frac{A_{ij}}{r_{ij}^6} + \frac{B_{ij}}{r_{ij}^{12}} \right) \right]$$

where A^{HB} and B^{HB} have been derived by fitting to ab initio SCF results on small molecule interactions (see Ref. 39). ($\theta = (MH, HN)$ for the hydrogen bond M–H $\cdots$ N). Beyond $\theta = 90°$ or beyond H $\cdots$ N = 6 Å, the normal Lennard-Jones term is employed.

The third term in Eqn. A-1 accounts for the torsional or anomeric potentials around single bonds *S* with dihedral angles τ_S: n_S is the multiplicity of the torsional potential and V_S is the height of the potential barrier, the parameters employed having been derived in our laboratory from experimental values and quantum chemical calculations (see Ref. 39).

The energy optimization procedure employs a conjugate gradient minimizer, using the BFGS algorithm [44], which uses analytical energy derivatives, requiring the analytical calculation of the forces and torques acting on each atom of the system.

The conformational study with optimization of all dihedral angles of the sequence Asn-Val-Ile-Ile-Pro-Lys embedded in an α-helix made otherwise of alanines was carried out using a method derived [45] from that described above to allow for the flexibility of rings in an energy optimization procedure, a necessity imposed by the presence of the proline residue. In the method used (CINFLEX, standing for constrained internal coordinate flexibility), the variables describing the conformation of the rings are limited to dihedral and ring valence angles and the ring closure conditions are treated as equality constraints. The ring can be described by a set of independent and dependent valence angles and independent and dependent dihedral angles. This method allows the backbone dihedral angle ϕ of the proline residue, included in the ring, to be treated as an independent variable. The angle distortion force constants used in CINFLEX have been developed by fitting to ab-initio calculations (for their values, see Ref. 45).

The examination of the existence or absence of Van der Waals contacts between two molecules A and B involves energy calculations of their Lennard-Jones interaction. This is computed using the second term of Eqn. A-1 this time summed over all pairs of atoms *ij*, *i* belonging to A and *j* belonging to B. When this term for a given pair of atoms *ij* (*i* on A, *j* on B) is greater than 5 kcal/mol the two atoms implied are considered to be in close contact. Among such contacts found

between CPZ and different bundles, two extreme cases were differentiated: (i) one involving large values of the ij (i on CPZ, j on one helix) Lennard-Jones term whatever the orientation of CPZ, and which are unlikely to be removed upon a simple change in the conformation of the side chain implied in the contact but would instead require a significant change in the position of the helix involved; the corresponding structures were thus eliminated for too much contact; (ii) the other involving relatively smaller values of this term (between 5 and 10 kcal/mol), for which the contact between the atoms implied can obviously be removed by a slight conformational change of the side chain involved and/or a very small rotation or displacement of the helix. In such a situation the structure is not rejected since it is clear that the contact would disappear upon complete energy optimization.

References

1 Reynolds, J.A. and Karlin, A. (1978) Biochemistry 17, 2035–2038.
2 Lindstrom, J., Merlie, J. and Yogeeswaran, G. (1979) Biochemistry 18, 4465–4470.
3 Raftery, M.A., Hunkapiller, M.W., Strader, C.D. and Hood, L.E. (1980) Science 208, 1454–1457.
4 Brisson, A. and Unwin, P.N.T. (1985) Nature 315, 474–477.
5 Hucho, F. (1986) Eur. J. Biochem. 158, 211–226.
6 Toyoshima, C. and Unwin, N. (1988) Nature 336, 247–250.
7 Kubalek, E., Ralston, S., Lindstrom, J. and Unwin, N. (1987) J. Cell. Biol. 105, 9–19.
8 Claudio, T., Ballivet, M., Patrick, J. and Heinemann, S. (1983) Proc. Natl. Acad. Sci. USA 80, 1111–1115.
9 Devillers-Thiery, A., Giraudat, J., Bentaboulet, M. and Changeux, J.P. (1983) Proc. Natl. Acad. Sci. USA 80, 2067–2071.
10 Noda, M., Takahashi, H., Tanabe, T., Toyosato, M., Kikyotani, S., Furutani, Y., Hirose, T., Takashima, H., Inayama, S., Miyata, T. and Numa, S. (1983) Nature 302, 528–531.
11 Popot, J.L. and Changeux, J.P. (1984) Physiol. Rev. 64, 1162–1239.
12 Guy, H.R. (1984) Biophys. J. 45, 249–261.
13 Finer-Moore, J. and Stroud, R.M. (1984) Proc. Natl. Acad. Sci. USA 81, 155–159.
14 Hucho, F., Oberthur, W. and Lottspech, F. (1986) FEBS Lett. 205, 137–142.
15 Ratnam, M., Le Nguyen, D., Rivier, J., Sargent, P.B. and Lindstrom, J. (1986) Biochemistry 25, 2633–2643.
16 McCrea, P.D., Popot, J.L. and Engelman, D.M. (1987) EMBO J. 6, 3619–3626.
17 Di Paola, M., Czajhowski, C., Bodkin, M. and Karlin, A. (1988) Neurosci. Abstr. 114, 640.
18 Giraudat, J., Dennis, M., Heidmann, T., Chang, J.Y. and Changeux, J.P. (1986) Proc. Natl. Acad. Sci. USA 83, 2719–2723.
19 Changeux, J.P. and Revah, F. (1987) Trends NeuroSci. 10, 245–249.
20 Imoto, K., Methfessel, C., Sakmann, B., Mishina, M., Mori, Y., Konno, T., Fukuda, K., Kurasaki, M., Bujo, H., Fujita, K. and Numa, S. (1986) Nature 324, 670–674.
21 Giraudat, J., Dennis, M., Heidmann, T., Haumont, P.Y., Lederer, F. and Changeux, J.P. (1987) Biochemistry 26, 2410–2418.
22 Revah, F. and Changeux, J.P. (1988) in Transport through Membranes: Carriers, Channels and Pumps (Pullman, A., Jortner, J. and Pullman, B., eds.), pp. 321–335, Kluwer Academic Publishers (The Netherlands).
23 Furois-Corbin, S. and Pullman, A. (1988) in Transport through Membranes: Carriers, Channels and Pumps (Pullman, A., Jortner, J. and Pullman, B., eds.), pp. 337–357, Kluwer Academic Publishers (The Netherlands).
24 Imoto, K., Busch, C., Sakmann, B., Mishina, M., Konno, T., Nakai, J., Bujo, H., Mori, Y., Fukuda, K. and Numa, S. (1988) Nature 335, 645–648.
25 Heidmann, T., Oswald, R.E. and Changeux, J.P. (1983) Biochemistry 22, 3112–3127.
26 McDowell, J.J.H. (1969) Acta Cryst. B25, 2175–2181.
27 Ponder, J.W. and Richards, F.M. (1987) J. Mol. Biol. 193, 775–791.
28 Arnott, S. (1967) J. Mol. Biol. 30, 209–212.
29 Sundaralingam, M., Sekharudu, Y.C., Yathindra, N. and Ravichandran, V. (1987) Proteins: Structure, Function, and Genetics 2, 64–71.
30 Hilgenfeld, R. and Hucho, F. (1988) in Transport through Membranes: Carirers, Channels and Pumps (Pullman, A., Jortner, J. and Pullman, B., eds.), pp. 359–367, Kluwer Academic Publishers (The Netherlands).
31 Giraudat, J., Montecucco, C., Bisson, R. and Changeux, J.P. (1985) Biochemistry 24, 3121–3127.
32 Dani, J.A. (1988) in Transport through Membranes: Carriers, Channels and Pumps (Pullman, A., Jortner, J. and Pullman, B., eds.), pp. 297–319, Kluwer Academic Publishers (The Netherlands).
33 Cox, R.N., Kaldany, R.R., DiPaolo, M. and Karlin, A. (1986) J. Biol. Chem. 260, 7086–7193.
34 Karlin, A., Kao, P.N. and DiPaola, M. (1986) Trends Pharmacol. Sci. 7, 304–308.
35 Dani, J.A. and Eisenman, G. (1987) J. Gen. Physiol. 89, 959–983.
36 Piela, L., Nemethy, G. and Scheraga, H.A. (1987) Biopolymers 26, 1587–1600.
37 Furois-Corbin, S. and Pullman, A. (1988) Biochim. Biophys. Acta 944, 399–413.
38 Leonard, R.J., Labarca, C.G., Charnet, P., Davidson, N. and Lester, H.A. (1988) Science 242, 1578–1581.
39 Lavery, R., Sklenar, H., Zakrzewska, K. and Pullman, B. (1986) J. Biomol. Struct. Dyn. 3, 989–1014.
40 Zakrzewska, K. and Pullman, A. (1985) J. Comp. Chem. 6, 265–273.
41 Hückel, E.P. (1932) Z. Phys. 76, 728.
42 Del Re, G. (1958) J. Chem. Soc. 4031.
43 Zhurkin, V.B., Poltiev, V.I. and Florent'ev, V.L. (1980) Molekulyarnaya Biologiya 14, 116.
44 Powell, M.J.D. (1975) Report CSS, 15 A.E.R.E. Harwell, Harwell Library, Routine VA13A.
45 Lavery, R., Parker, I. and Kendrick, J. (1986) J. Biomol. Struct. Dyn. 4, 443–462.